Egyptian Journal of Biophysics and Biomedical Engineering
https://ejbbe.journals.ekb.eg/

A Simulation Study: Radiation Shielding Performance of Dy/Eu-Doped Boro-FBi Glasses

Abdelmoneim Saleh [a] and **B. M. Mahmoud** [b,*]

[a] *Basic Science Department, Higher Technological Institute, 10th of Ramadan City, 228, Egypt*
[b] *Physics Department1, Faculty of Science, Sohag University, Egypt*

The purpose of the present study is to investigate the effect of varying Bi_2O_3 and Al_2O_3 concentrations on gamma-ray and neutron shielding properties of glass. Five different glass samples with chemical composition $50B_2O_3$-(25-x)Al_2O_3-10Na_2O-xBi_2O_3-15CaF_2-0.5Dy_2O_3-0.5Eu_2O_3 where x = 5, 10, 15, 20, and 25 mol% are considered. The physical characteristics of the considered glasses, such as molar volume and atomic packing density, are calculated. The Monte Carlo N-Particle Transport Code (MCNP5) and XCOM software have been used to perform theoretical calculations for studying the shielding properties, such as the mass attenuation coefficient (MAC), half-value layer (HVL), mean free path (MFP), and neutron removal cross-section (RCS) in the energy range of 15-15000 keV. Increasing the Bi_2O_3 concentration significantly enhances all the aforementioned properties, making the S5 glass sample the most effective among the tested compositions. It provides complete protection against X-rays. Compared to other shielding materials, this glass sample is identified as a high-performance gamma-ray and neutron shield, making it suitable for radiation protection.

Keywords: Radiation protection, Boro-FBi glasses, Shielding properties, MCNP5, Mass attenuation coefficient.

Introduction

Many previous studies have been concerned with how to reduce the risk of radiation exposure, as when a biological system is exposed to nuclear radiation, it causes serious dangers. The growing application of nuclear technology in healthcare, industrial, and energy sectors has generated considerable apprehension regarding radiation safety. Consequently, there is an ongoing necessity to investigate and create improved materials that provide effective radiation shielding. The quest for materials that offer superior shielding efficacy while satisfying structural, environmental, and economic standards has emerged as a global research priority.

Gamma-ray and neutrons are two types of ionizing radiation that are especially hard to deal with, as they can pass through materials very easily. Gamma-ray need thick materials to lower their intensity adequately. Neutrons, on the other hand, do not have an electrical charge and interact with matter in a completely different way[1].

Traditional defensive substances, including concrete and lead (Pb), have been the backbone of radiation protection techniques across various industries. Lead, with its noticeably high density and atomic number, serves as a good barrier against gamma rays and X-rays by absorbing a significant portion of their energy. Concrete is a better choice for radiation shielding because it is less expensive and can be shaped in various ways. Although concrete and lead are more effective at blocking radiation, they have limitations in terms of density, mechanical properties, and neutron shielding [2]. As a result, there is a growing interest in creating new materials that offer better shielding, especially those that are easy to manufacture, possess strong mechanical properties, and exhibit high attenuation.

Recently, various materials have demonstrated good shielding properties, including glasses, ceramics, and composites [3-6]. Glasses exhibit an exceptional combination of physical and chemical characteristics, rending them remarkably appropriate for radiation protection. These residences consist of high optical transparency, which allows for visibility and monitoring during radiation exposure; pretty high density, which contributes to effective attenuation of ionizing radiation; sizable hardness and fracture longevity, supplying mechanical sturdiness beneath pressure; and awesome resistance to thermal shock, enabling them to face up to rapid temperature modifications without cracking or degradation. The intrinsic characteristics of glass substances are

*Corresponding author e-mail: b.elyan@science.sohag.edu.eg
Received: 14/05/2025; Accepted: 28/06/2025
DOI: 10.21608/EJBBE.2025.384642.1084

strongly influenced by their chemical composition and the specific conditions under which they are processed, which include melting temperature, cooling rate, and the incorporation of numerous dopants or heavy metal oxides. By carefully adjusting these settings, you may get the best performance, mechanical strength, and shielding efficiency from glass-based materials. Additionally, glasses are superior to other shielding materials due to their affordability, ease of manufacture, and environmental friendliness [7, 8].

Many studies have emphasized the significance of doping glass with heavy oxides to enhance its radiation shielding capabilities and augment its radiative capacity [9-12]. This makes them good for places where both safety and visibility are important. The adaptability in glass composition enables researchers to tailor materials for specific shielding purposes by adjusting the types and concentrations of dopants. Susoy et al. investigated the impact of incorporating Cr_2O_3 into LiF-SrO-B_2O_3 glasses, which enhanced the shielding characteristics while diminishing the glass's transparency [13]. Heavy metal oxide glasses containing heavy metal atoms with high atomic numbers, such as Bi, are effective at blocking gamma-ray. These glasses are considered a good option for systems that protect against radiation. A previous study investigated the effect of Bi_2O_3/Pbo additives on lead-zinc-tellurite glasses [14]. They discovered that glasses containing a Bi_2O_3 addition provide enhanced protection against ionizing radiation, with the shielding effectiveness improving as the Bi_2O_3 concentration rises.

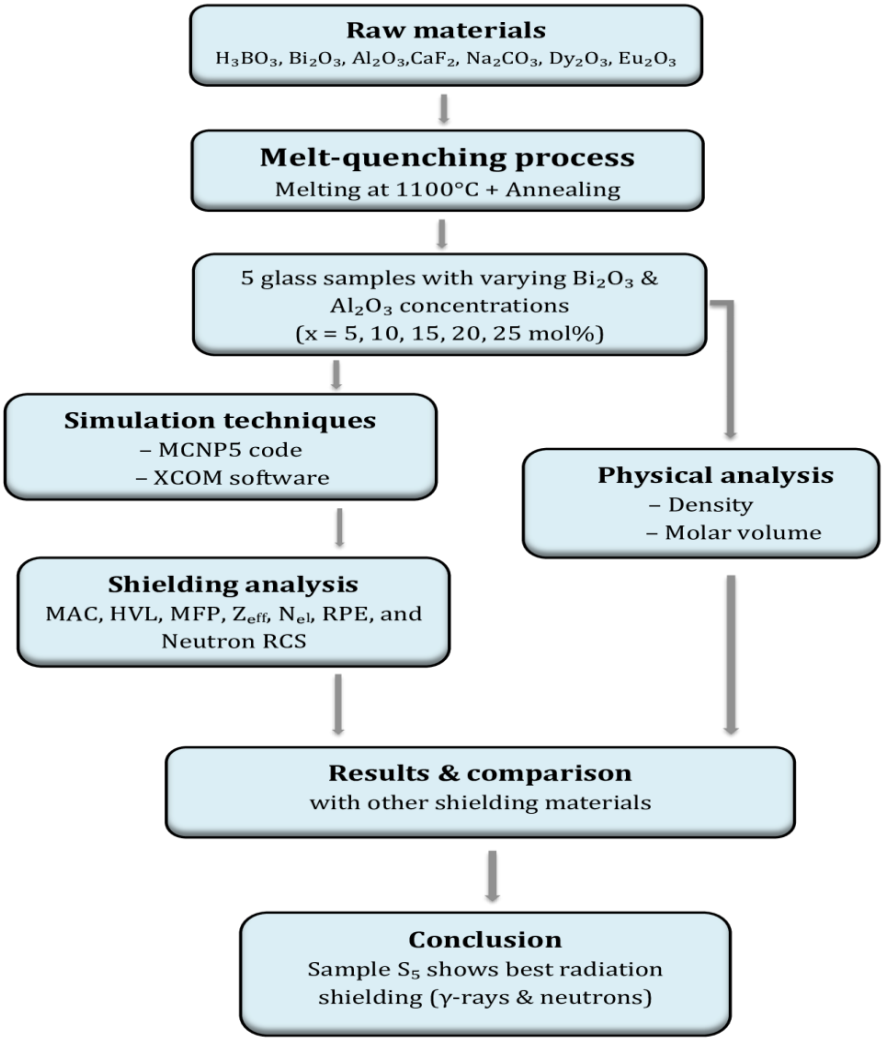

Fig. 1. Schematic overview of the study workflow and materials used.

The combination of elements that can absorb many neutrons, like boron, can also improve the shielding properties of neutrons. Singh et al. [15, 16] assessed the radiation-shielding properties of boron-doped materials. Fluorine can alter the structure of glass and increase its chemical stability due to its low atomic number and high electronegativity. Due to its distinctive features, borofluorbismuth (Boro-FBi) glasses have garnered considerable attention. Adding rare-earth elements like dysprosium (Dy) and europium (Eu) to Boro-FBi glasses can enhance their ability to block radiation. Dy has a large neutron absorption cross-section and a large thermal neutron capture cross-section, which makes it much better at shielding neutrons. Eu glows in the dark, which makes it useful as a radiation detector.

Additionally, the combination of Dy and Eu in the glass composition not only enhances its ability to block neutrons but also enables the creation of materials that can both protect against radiation and monitor it in real time. This synergistic action makes the glass more thermally stable and mechanically robust overall, making it ideal for demanding nuclear and industrial applications. We decided to focus our work on Boro-FBi glasses doped with Dy/Eu, as discussed earlier.

The flowchart in Fig. 1 illustrates the primary steps of the methodology employed in this study. It begins with the selection and preparation of raw materials, followed by the melt-quenching process conducted at 1100 °C with subsequent annealing. Five glass samples were then fabricated with varying concentrations of Bi_2O_3 and Al_2O_3 . The study proceeds with simulation analyses using MCNP5 code and XCOM software to evaluate radiation interaction parameters. Physical characterization of the samples includes measurements of density and molar volume. Furthermore, the shielding performance of each sample is analyzed through key indicators, including MAC, HVL, MFP, Z_{eff}, N_{el}, RPE, and neutron RCS. The results are compared with existing shielding materials, leading to the conclusion that sample S_5 demonstrates the most effective radiation shielding capabilities.

The results of this study will provide us with useful information on Boro-FBi glasses doped with Dy/Eu, which are used as sophisticated radiation shielding materials. This information will be useful for developing more effective shielding materials for hospitals, nuclear power plants, and other facilities that utilize ionizing radiation.

Material and methods

A series of glasses with the chemical composition $50B_2O_3$-(25-x)Al_2O_3-10Na_2O-xBi_2O_3-15CaF_2-0.5Dy_2O_3-0.5Eu_2O_3 where x = 5, 10, 15, 20, and 25 mol% had been formerly synthesized via the melt quenching method [17] to study their physical characteristics and shielding effectiveness against radiation. The choice of oxides was made with great care to fit the study's specific goals. The main oxides studied in this research, known as glass modifiers, were bismuth oxides (Bi_2O_3). These oxides have a significant impact on the structural, optical, and thermal properties of the glass samples, rendering them essential for attaining the desired material attributes. Thus, it is necessary to achieve the desired material qualities. The research employed powders of H_3BO_3, Bi_2O_3, Al_2O_3, CaF_2, Na_2CO_3, Dy_2O_3, and Eu_2O_3 as fundamental materials. We measured out 20 grams of each material and placed them in a mortar to grind and blend them according to the given ratios. Then, the mixture was transferred to a muffle furnace, where it underwent heating at a constant rate of 10°C per minute until reaching 1100°C, maintaining this temperature for 60 minutes to achieve complete melting. The hot liquid was quickly poured into a steel mold in the shape of a rectangle, and it underwent annealing at 450 °C for one hour. The fabricated glass samples were subjected to various performance and structural evaluations, including cutting and polishing.

Simulation techniques

1. XCOM program

XCOM software program is recognized as one of the pioneering and most dependable web-based gear for calculating the MAC of substances exposed to photon radiation. The National Institute of Standards and Technology (NIST) created and maintains XCOM, which enables researchers to model the interaction of photons over a wide range of energies (from 1 keV to 100 GeV). This makes it an important tool for research on radiation shielding [18]. Users can input either chemical formulas or elemental weight fractions, allowing for the investigation of both pure elements and complex compounds or mixtures, including glasses and composites. The application retrieves pertinent cross-sectional data from an extensive online database, ensuring precise and up-to-date calculations.

This study utilized the elemental weight percentages of each synthesized glass sample as input for the XCOM platform to compute the MAC values. These coefficients are essential for assessing the photon attenuation efficacy of materials, as they quantify the likelihood of photon interaction per unit mass. XCOM calculates the MAC based on established photon interaction mechanisms, including the Compton scattering, photoelectric effect, and pair production, contingent upon the energy level. The HVL and MFP, which depend on both the density of the material and the MAC, cannot be obtained directly from XCOM. Instead, they must be calculated externally using other mathematical relationships or specialized software tools [19].

Integrating the results from XCOM with supplementary computational approaches yields a more comprehensive understanding of the shielding efficacy of each glass sample, thereby facilitating the design of optimal radiation shielding materials.

2. MCNP5 code

It is widely acknowledged that mathematical methods, such as Monte Carlo simulations, are well-established as essential tools for addressing a wide range of physical problems. These simulation techniques operate by

incorporating the physical and geometric characteristics of the equipment used, as well as cross-sectional data and various databases referenced in experimental studies. MCNP5 simulations are commonly used to evaluate the radiation shielding effectiveness of various glass compositions [20-23].

The MAC evaluation of the synthesized Boro-FBi glass sample is performed by using the MCNP5 code based on Lambert-Beer law [24]. The simulation setup is illustrated as a three-dimensional model created using the visual editor, as shown in Fig. 2. The simulation setup comprises main elements, including an isotropic point radiation source and a lead collimator system. The glass sample is placed between the radiation source and an F4 tally mesh detector, accompanied by a lead shield that inhibits radiation scattering [19]. The MAC is determined using the linear attenuation coefficient (LAC) and material densities across various photon energy levels.

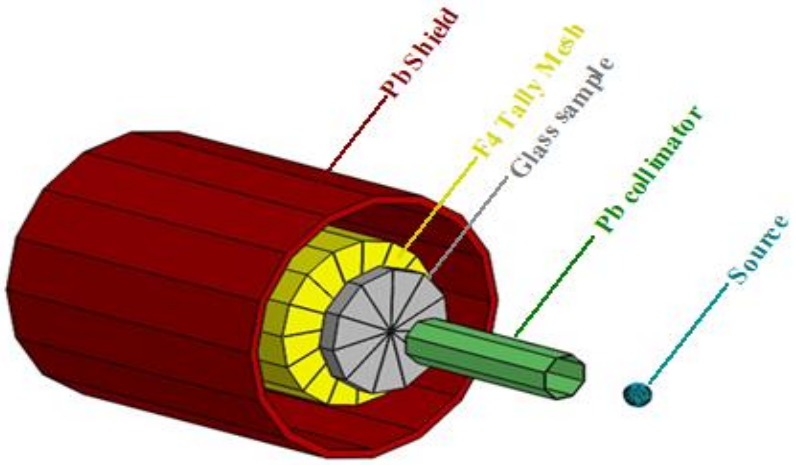

Fig. 2. Gamma-ray attenuation setup of MCNP5's visualization tool.

3. Basic relations of shielding parameters

The gamma-ray intensity is exponentially decreased by the attenuation law (Beer-Lambert law), which illustrates how gamma-ray photons are progressively absorbed or scattered by the atoms in the shielding material [24]:

$$\frac{I}{I_0} = e^{-\mu x} \tag{1}$$

Where I_0 represents the initial radiation intensity prior to attenuation, and I denotes the intensity after transmission via the material. The parameter μ corresponds to the LAC, while x represents the sample thickness.

The MAC represents the likelihood of photons interacting with a given material. Theoretically, MAC can be determined using the following relation [25, 26]:

$$MAC = \mu_m = \frac{\mu}{\rho} = \frac{1}{x}\ln\left(\frac{I_0}{I}\right) \tag{2}$$

Where ρ is the material density.

The determination of MAC values was obtained through the utilization of previously discussed programs. The percentage difference (Diff %) between the two calculated MAC values is expressed by:

$$Diff(\%) = \frac{|(\mu/\rho)_{MCNPX} - (\mu/\rho)_{XCOM}|}{(\mu/\rho)_{MCNPX}} \tag{3}$$

HVL is a major shielding parameter, where the material's thickness when incident photon intensity is reduced to 50% of the initial value [27]:

$$HVL = \frac{\ln(2)}{\mu} \tag{4}$$

The mean free path (MFP) is defined as the average distance that gamma-ray traverse between two consecutive interactions and the shielding material and is expressed by MFP

$$MFP = \frac{1}{\mu} \tag{5}$$

The effective atomic number (Z_{eff}) is used to understand the attenuation properties of a compound. Thus, this parameter represents a weighted mean of the atomic numbers of the constituent elements of the glass composition, which depends on the characteristic interaction of the material with radiation. This parameter is obtained by [17]:

$$Z_{eff} = \frac{\sum_i n_i A_i (\frac{\mu}{\rho})_i}{\sum_i n_i A_i / Z_i (\frac{\mu}{\rho})_i} \quad (6)$$

Where n_i and A_i are the number of atoms and the atomic weight of the element i.

The number of electrons per gram, which is called electron density N_{el}, is calculated using Z_{eff} by [25]:

$$N_{el} = \frac{Z_{eff} N_A \sum_i n_i A_i (\frac{\mu}{\rho})_i}{M} \quad (7)$$

Where N_A is the Avogadro's number.

Radiation protection power (RBE) is the effectiveness of a material in weakening ionizing radiation to determine its shielding capability. By knowing I_0 and I values, RBE is calculated as:

$$\text{RBE (\%)} = \left(1 - \frac{I}{I_0}\right) x100 \quad (8)$$

From the above-mentioned fundamental physical quantities, the removal cross-section (RCS) (Σ_R) is derived. It is an essential shielding parameter, defined as the probability of neutron interactions within a given homogeneous material. The $\Sigma_{R/\rho}$ values pertaining to each constituent element utilized in the glass formulation can be used to determine the effective RCS of the studied glass samples [28,29]:

$$\sum_{R/\rho} = \sum_i w_i (\sum_{R/\rho})_i \quad (9)$$

and

$$\sum_R = \sum_i \rho_i (\sum_{R/\rho})_i \quad (10)$$

Where ρ_i is the partial density within the glass sample for each element ($g.cm^{-3}$). In this study, the effective RCS was also clarified using the user-friendly Phy-X/PSD program [30].

Results and discussion

1. Physical properties

Table 1 presents the composition, density, and molar volume of the prepared glasses, with a chemical composition of $50B_2O_3$-(25-x) Al_2O_3-$10Na_2O$-xBi_2O_3-$15CaF_2$-$0.5Dy_2O_3$-$0.5Eu_2O_3$ where x = 5, 10, 15, 20, and 25 mol%. The chemical composition of the prepared glass samples (S1–S5) is illustrated in the stacked bar chart Fig. 3 (a). Each sample consists of a constant amount of B_2O_3 (49 mol%) and fixed concentrations of Na_2O (10 mol%), CaF_2 (15 mol%), Dy_2O_3 (0.5 mol%), and Eu_2O_3 (0.5 mol%). The main compositional variation lies in the relative proportions of Bi_2O_3 and Al_2O_3, where Bi_2O_3 increases from 5 to 25 mol% across samples S1 to S5, while Al_2O_3 correspondingly decreases from 20 to 0 mol%. This gradual substitution explores how Bi_2O_3 modifies the structural and physical characteristics of the glass samples.

Table 1. Glass compositions, density, and molar volume for the studied glasses.

Glass code	Chemical composition (mol%)							Density (g/cm^3)	Molar volume (cm^3/mol)
	B_2O_3	Bi_2O_3	Al_2O_3	Na_2O	CaF_2	Dy_2O_3	Eu_2O_3		
S1	49	5	20	10	15	0.5	0.5	3.14	31.961
S2	49	10	15	10	15	0.5	0.5	3.61	32.769
S3	49	15	10	10	15	0.5	0.5	3.99	34.167
S4	49	20	5	10	15	0.5	0.5	4.345	35.565
S5	49	25	--	10	15	0.5	0.5	4.61	37.41

The density of the samples studied increased from 3.14 to 4.61 g/cm^3 (Fig.3 (b)) as the Bi_2O_3 content increased from 5 to 25 mol%. The increase in density is related to the significant increase in molar volume values, from 31.961 to 37.41 cm³/mol. This is because the lighter oxide (Al_2O_3, with a density of 3.99 g/cm^3) is replaced by a heavier oxide (Bi_2O_3, with a density of 8.9 g/cm^3), resulting in a denser glass system. The corresponding increase of the molar volume values from 31.961 to 37.41 cm^3/mol is due to the small size of the aluminum ions compared to the size of the bismuth ions. In addition, bismuth tends to form weaker bonds with oxygen compared to aluminum, and this weakness in the bonds contributes to increasing the distance between the ions in the lattice and increasing the molar size.

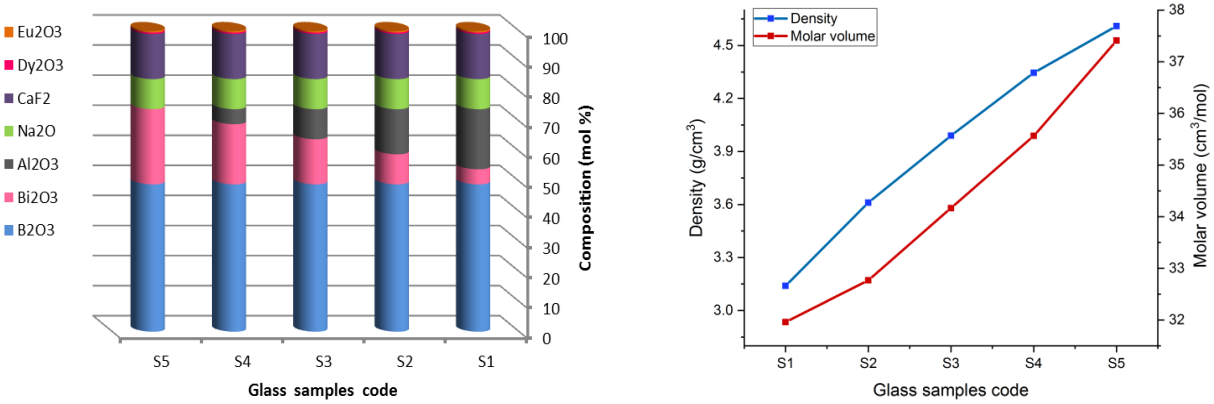

Fig. 3. Stacked bar chart (on the left) showing the chemical composition (in mol%) of the studied samples S1–S5, comprising B_2O_3, Bi_2O_3, Al_2O_3, Na_2O, CaF_2, Dy_2O_3, and Eu_2O_3. The line graph on the right illustrates the variation of density (g/cm³) and molar volume (cm³/mol) as a function of glass composition.

2. The Shielding Properties

A gamma shielding study was carried out by calculating the MAC values for the considered glass samples. MAC values are strongly related by the photon energies through various mechanisms (Compton scattering, pair production, and photoelectric effect) [31]. Theoretical calculations were performed using the MCNP5 simulation and the XCOM program.

Figure 4 shows the MAC values as a function of photon energy. It is clear that the five glass samples exhibit the same behavior; MAC values decrease as the photon energy increases from 0.015 to 15 MeV, and two peaks are observed at the same energies. The MAC values rise as Al_2O_3 is substituted with Bi_2O_3 since the probability of photon interactions increases with the atomic number of the constituent elements. The first peak is due to Rayleigh scattering, which depends on the glass polarizability. The second peak, which appears at approximately 0.1 MeV, represents the absorption edge of the K-absorption edge in Bi. The k-absorption edge shows a sharp increase in the MAC due to the photoelectric effect, where photons have enough energy to eject K-shell electrons. Below the K-edge, the attenuation is primarily due to Compton scattering and photoelectric absorption in higher shells (L, M, etc.). Above the K-edge, the attenuation remains high but may start to decrease slightly as other interaction mechanisms, like pair production, become significant at higher energies. Comparing these values with those obtained from the NIST for bismuth can validate the observed trends. The free Al_2O_3 sample (encoded S5) has the greatest MAC values and, therefore, is the most resistant to gamma radiation. The matching between the MCNP5 and XCOM data indicates that the MCNP5 simulation is the correct choice for calculating MAC values.

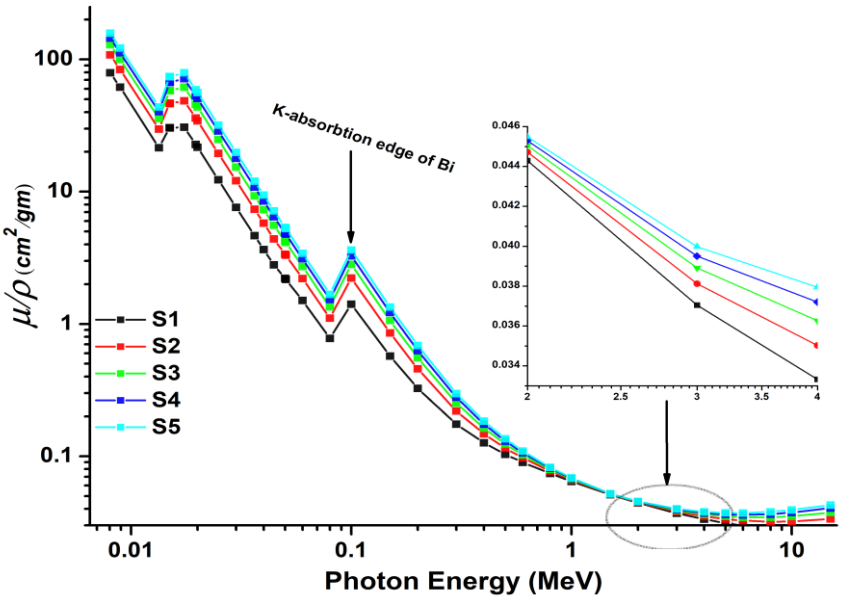

Fig. 4. The MAC as a function of the photon energy(Dots represent the MCNP5 simulation, and the line represents XCOM).

The HVL calculations are displayed in Fig. 5 as a function of the photon energy. At low energies (e.g., 10 keV), the HVL is relatively low, indicating that less thickness is required to attenuate the radiation. HVL values increase with both increasing photon energy and bismuth oxide concentration. This behavior happens since as the gamma-ray energy increases, more photons penetrate the glass. The variation in HVL values of the considered glasses is small at low energies, up to 0.1 MeV, and increases significantly at energies higher than 1 MeV. In contrast to the MAC-energy curve, the free Al_2O_3 sample (S5) has the smallest HVL values among the other samples. Therefore, this sample is more efficient at retaining photons and exhibits the best shielding performance.

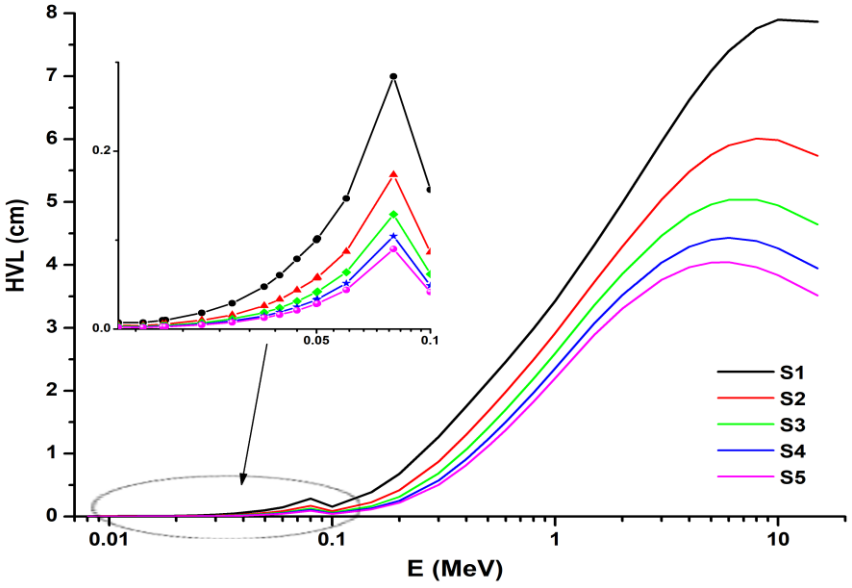

Fig. 5. HVL values as a function of the photon energy (dots represent the MCNP5 simulation, and the line represents XCOM).

MFP is a crucial parameter in designing radiation shields; it helps scientists determine how effectively a material can attenuate gamma radiation in various applications. A reduced MFP signifies that the material is more proficient in attenuating gamma radiation, which is crucial for minimizing exposure and guaranteeing safety. Scientists use MFP values to assess the shielding efficacy of various materials and refine the thickness and composition of protective barriers for specific purposes. In medical imaging facilities, it is crucial to utilize materials with low MFP values to protect patients and healthcare personnel from excessive radiation exposure. In nuclear power plants or radioactive waste storage facilities, utilizing materials with optimal mean free path

values ensures operational safety and structural integrity. Figure 6 presents a comparison of the MFP values of the S5 sample with conventional shielding materials (such as Ordinary concrete, Ilmenite limonite, Basalt magnetite, Ilmenite concretes Hematite Serpentine, and Barite [32]) and some recently studied glasses and polymer (such as RS-360 glass [33], Guanine nucleobase [34], VR2 and VR3 volcanic rocks [35], MASLN4 [36], PSS5 [37], LTM-C [38], Ca/Pb-BBC4 [39], T1 [40], PCNK60 [41], SLGC-E5 [42], LBZ4 [43], SBC-B35 [44], P2 polymer [45], TL5 [46], and BBSN5.7 [47]) at 0.662, 1.173, 1.33 and 2.506 MeV. It was observed that the MFP value increases with photon energy for all materials. Except for RS-360 at 2.506 MeV, the S5 sample exhibits the lowest MFP value, indicating superior gamma-ray shielding performance.

Figures 7 and 8 show the variations of the Z_{eff} and N_{el} with photon energy for the glass samples studied. The curves of Z_{eff} and Nel are expected to have the same behavior as a function of increasing photon energy as described in Equations (6) and (7). The values of both Z_{eff} and N_{el} increase with the higher Bi_2O_3 concentration. The values of both parameters increase at lower photon energies due to the predominant influence of the photoelectric effect. Around 0.1 MeV, there is a noticeable peak, which is due to the K shell absorption edge of bismuth. Above this point, Z_{eff} and N_{el} sharply reduce with increasing photon energy, mainly because of the effect of the Compton scattering cross-section. However, both parameters increase again at energies exceeding about 3 MeV, which is attributed to the commencement of the pair production mechanism.

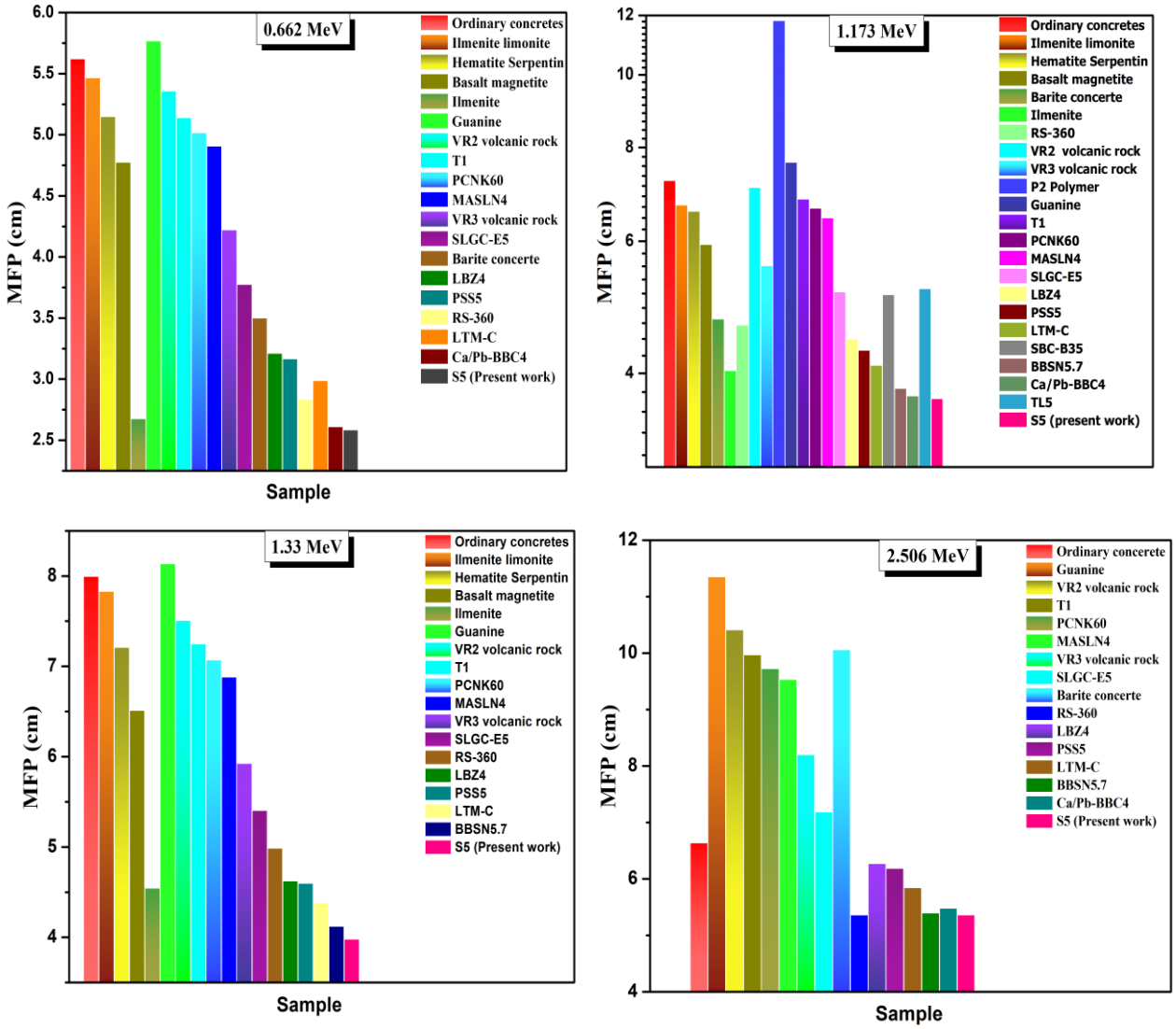

Fig. 6. Comparison of the MFP values of the studied sample with conventional shielding materials and other recently examined glasses and polymers at energies of 0.662, 1.173, 1.33, and 2.506 MeV.

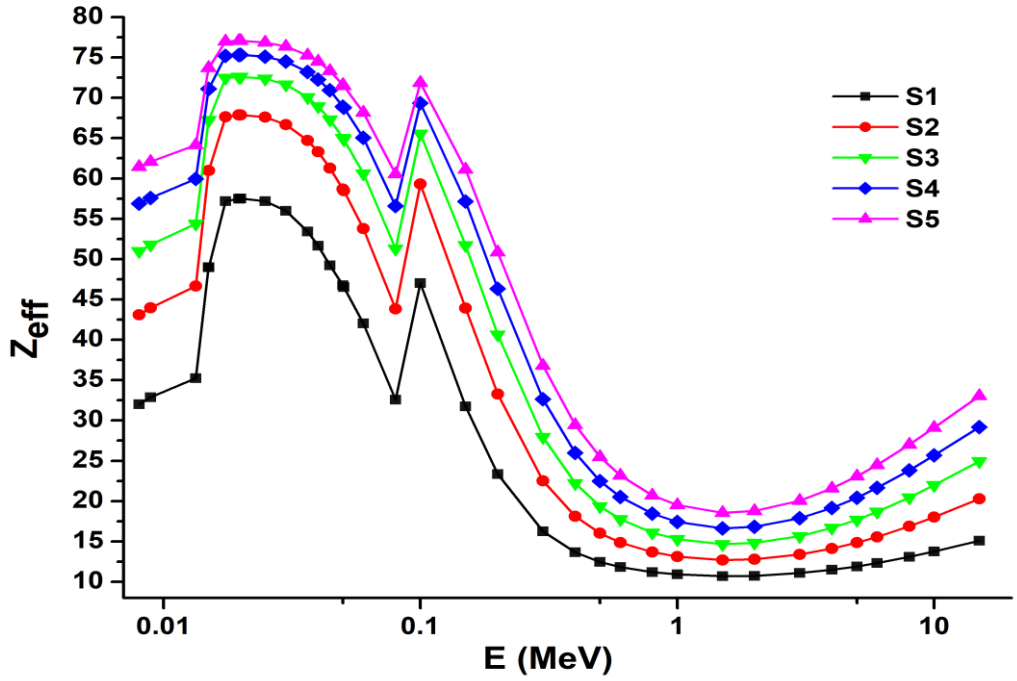

Fig. 7. Z_{eff} values as a function of the photon energy (Dots represent the MCNP5 simulation, and the line represents XCOM).

RBE, which is determined using eq. (8) is a measure of a shield's ability to absorb or scatter radiation. It represents the percentage reduction in radiation intensity after passing through a specific material thickness. A higher RPE value indicates a more effective shielding material. Fig. 9 displays the RBE versus photon energy for the considered samples. The S5 sample gives complete protection (100%) against X-rays within the energy range of 15-150 keV; above 150 keV, the efficiency decreases significantly with the increase in photon energy. This reflects the effective increase in the Bi2O3 concentration. Therefore, the sample S5 is an ideal material for X-rays protection.

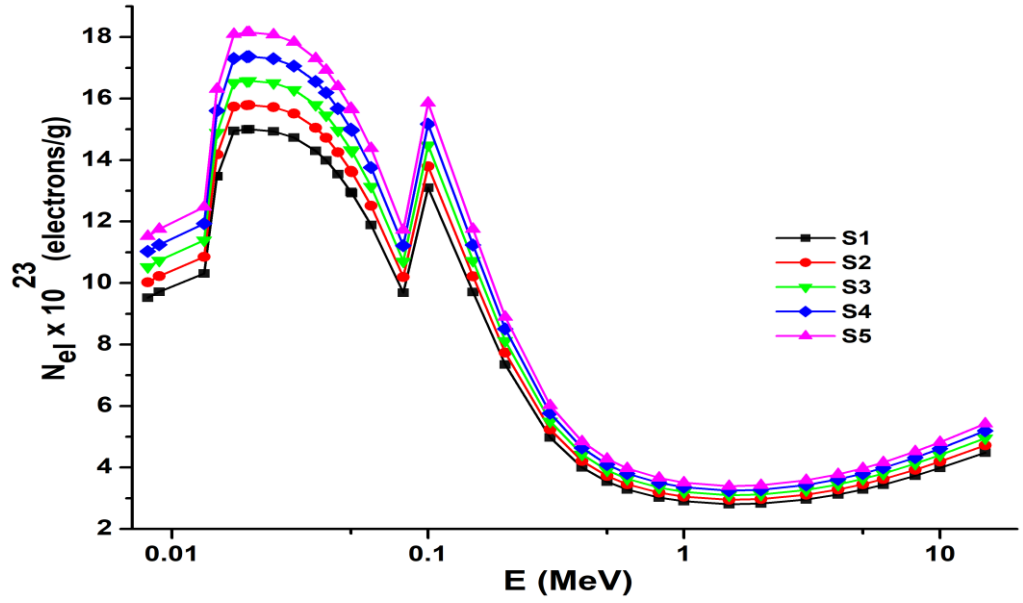

Fig. 8. N_{el} values as a function of the photon energy (Dots represent the MCNP5 simulation, and the line represents XCOM).

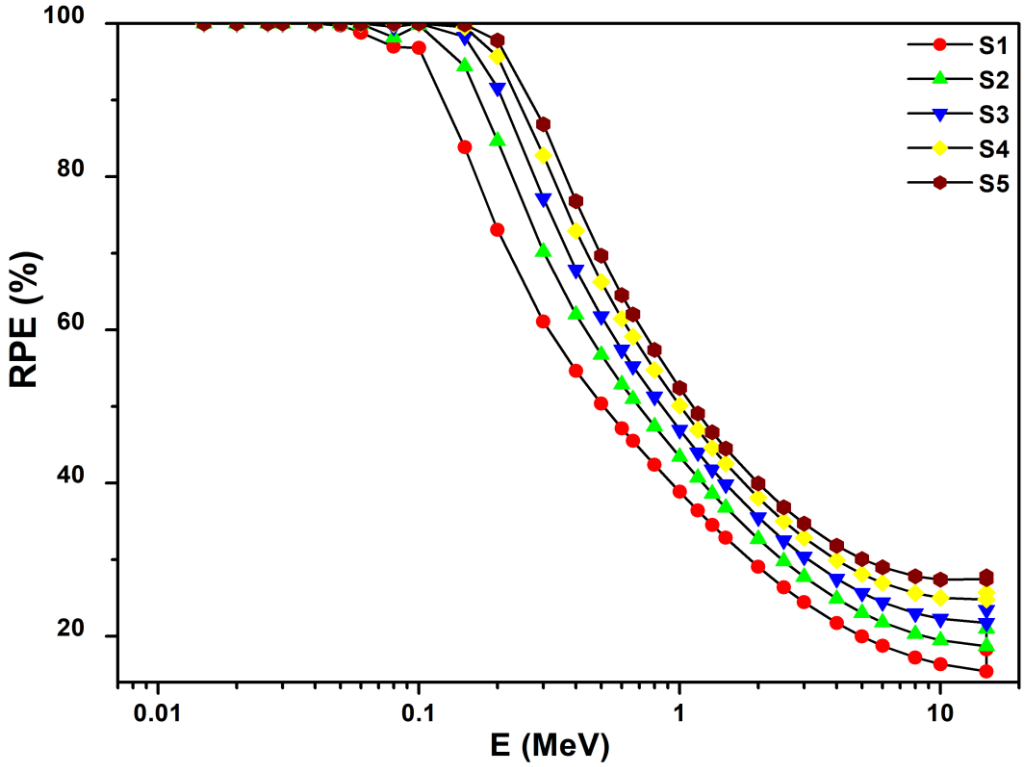

Fig. 9. RPE values as a function of the photon energy (Dots represent the MCNP5 simulation, and the line represents XCOM).

It is well known that fast neutrons are utilized in various applications, making it crucial to investigate methods for attenuating them. Among all the samples considered, sample S5 showed the most acceptable values of MAC, HVL, MFP, Z_{eff}, N_{el}, and RPE. Therefore, calculations of the effective removal cross-section (RCS) were carried out only for this sample. The results of the RCS of fast neutrons in the S5 sample benchmarked against other commonly used neutron shielding materials and recently studied glass samples are shown in Fig. 10. We compare RCS values with graphite, water, ordinary concrete, basalt-magnetite, hematite serpentine, and hematite limonite. RCS varies significantly across different materials, reflecting their differing abilities to attenuate radiation. Graphite has relatively low RCS values, indicating poor shielding performance. Ordinary concrete, Ilmenite limonite, hematite serpentine, and basalt-magnetite have moderate values, making them suitable for general shielding applications. Water has a higher value, indicating better shielding performance.

It is clear that our sample is the best neutron shield material with the largest RCS value. The exceptional neutron attenuation capabilities of sample S5 indicate that glass composites infused with heavy metals and rare-earth elements possess considerable promise for practical radiation shielding applications. Moreover, their structural tunability enables the exact regulation of radiation interaction parameters. This is particularly crucial in settings where compact, lightweight, and multifunctional shielding is necessary, such as in space missions, nuclear medical imaging facilities, and portable radiation protection systems. The significant elimination cross-section noted in S5 renders it a viable alternative for substituting or augmenting traditional materials in essential shielding applications. The incorporation of Dy and Eu doping not only improves neutron absorption but may also facilitate dual functionality, including shielding and radiation detection, due to Eu's luminous characteristics. These findings create opportunities for the development of advanced shielding materials designed for particular radiation spectra and operating environments.

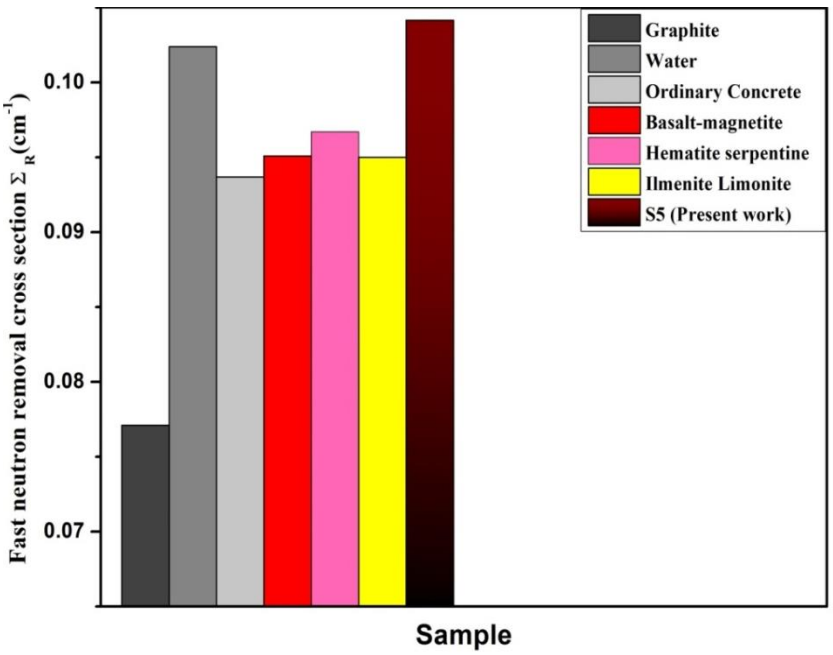

Fig. 10. RCS values of fast neutrons for the S_5 sample compared to that of other widely used neutron shielding materials.

Conclusion

In this work, we examine the variations in both physical and shielding characteristics that result from varying the concentrations of aluminum and bismuth oxides in a Boro-FBi glass doped with Dy/Eu. The prepared samples have the chemical composition $50B_2O_3$-(25-x) Al_2O_3-10Na_2O-xBi_2O_3-15CaF_2-0.5Dy_2O_3-0.5Eu_2O_3 where x = 5, 10, 15, 20, and 25 mol%. Physical and shielding properties have been determined, including molar volume, atomic packing density, MAC, HVL, MFP, Z_{eff}, N_{el}, RPE, and RCS. The MCNP5 code and the XCOM program were used to simulate the radiation shielding properties of the samples, and both gave completely identical results. The sample encoded S5, which is free from Al_2O_3 and contains a higher concentration of Bi_2O_3, exhibited the best values in all the studied properties. This finding highlights the crucial role of bismuth oxide as a glass modifier that enhances the glass shielding characteristics. Therefore, Bi is considered the best alternative to Pb in glass compositions.

In conclusion, the S5 sample (with a chemical composition $50B_2O_3$ -10Na_2O-25Bi_2O_3-15CaF_2-0.5Dy_2O_3-0.5Eu_2O_3) demonstrates excellent gamma and neutron shielding properties, making it a promising candidate for radiation protection applications.

Declarations

Acknowledgments: We would like to express our gratitude to all those who contributed to the success of this research.

Statement of funding: This study did not obtain any financial support.

Ethical approbation: Not applicable

Availability of data: Available

References

1. Wang, K., Ma, L., Yang, C., Bian, Z., Zhang, D., Cui, S., Wang, M., Chen, Z., & Li, X. (2023). Recent progress in Gd-containing materials for neutron shielding applications: A review. Materials, 16(12), 4305.
2. Eke, C., Agar, O., Segebade, C., & Boztosun, I. (2017). Attenuation properties of radiation shielding materials such as granite and marble against γ-ray energies between 80 and 1350 keV. Radiochimica Acta, 105(10), 851–863.
3. Aygün, B., Şakar, E., Cinan, E., Yorgun, N. Y., Sayyed, M. I., Agar, O., & Karabulut, A. (2020). Development and production of metal oxide doped glasses for gamma-ray and fast neutron shielding. Radiation Physics and Chemistry, 174, 108897.
4. Saleh, A., El-Feky, M. G., Hafiz, M. S., & Kawady, N. A. (2023). Experimental and theoretical investigation on physical, structure, and protection features of TeO_2–B_2O_3 glass doped with PbO in terms of gamma, neutron, proton, and alpha particles. Radiation Physics and Chemistry, 202, 110586.

5. Sayyed, M. I. (2025). Modulation of optical, mechanical and radiation shielding characteristics in TeO_2-B_2O_3–BaO–CeO_2 glasses with varying CeO_2 level. Optical Materials, 158, 116492.

6. Juhim, F., Chee, F. P., Awang, A., Salleh, S., Rumaling, M. I., Alalawi, A., & Al-Buriahi, M. S. (2025). Effect of Al_2O_3, RHF, and RHA on gamma shielding and mechanical properties of TeO_2-based glass using Phy-X/PSD. Progress in Nuclear Energy, 185, 105767.

7. Al-Buriahi, M. S., Kurtulus, R., Eke, C., Alomairy, S., & Olarinoye, I. O. (2024). An insight into advanced glass systems for radiation shielding applications: A review on different modifiers and heavy metal oxides-based glasses. Heliyon, 10(22).

8. Juhim, F., Chee, F. P., Awang, A., Duinong, M., Rasmidi, R., & Rumaling, M. I. (2022). Review—Radiation shielding properties of tellurite and silicate glass. Journal of Solid State Science and Technology, 11(7), 076006.

9. Kumar, A., Sayyed, M. I., Dong, M., & Xue, X. X. (2018). Effect of PbO on the shielding behavior of ZnO–P_2O_5 glass system using Monte Carlo simulation. Journal of Non-Crystalline Solids.

10. Al-Ghamdi, H., Almuqrin, A. H., Sayyed, M. I., & Kumar, A. (2021). The physical, structural, and gamma-ray shielding effectiveness of the novel Li_2O–K_2O–B_2O_3–TeO_2 glasses. Results in Physics, 29, 104726.

11. Saleh, A., Harqani, N. A., Al-Ghamdi, W., Osman, K. T., & Elshoukrofy, A. S. M. (2024). The role of MoO_3 on the physical, elasto-mechanical and nuclear shielding efficiency of barium-boro-bismuthate glass system: Comparative investigation. Materials Chemistry and Physics, 322, 129574.

12. Alharbiy, N., Khattari, Z. Y., Rammah, Y. S., & Saleh, A. (2023). Role of Al_2O_3, WO_3, Nb_2O_5, and PbO on the physical, elasto-mechanical, and radiation attenuation performance of borotellurite glasses. Journal of Materials Science: Materials in Electronics, 34(3), 191.

13. Susoy, G., Altunsoy Guclu, E. E., Kilicoglu, O., Kamislioglu, M., Al-Buriahi, M. S., Abuzaid, M. M., & Tekin, H. O. (2019). The impact of Cr_2O_3 additive on nuclear radiation shielding properties of LiF–SrO–B_2O_3 glass system. Materials Chemistry and Physics, 122481.

14. Al-Buriahi, M. S., El-Agawany, F. I., Sriwunkum, C., Akyıldırım, H., Arslan, H., Tonguc, B. T., El-Mallawany, R., & Rammah, Y. S. (2019). Influence of Bi_2O_3/PbO on nuclear shielding characteristics of lead–zinc–tellurite glasses. Physica B: Condensed Matter, 411946.

15. Singh, V. M., & Badiger, N. M. (2015). U-ray interaction characteristics for some boron-containing materials. Scientific Direct, 113, 24–27.

16. Levet, A., Kavaz, E., & Ozdemir, Y. (2020). An experimental study on the investigation of nuclear radiation shielding characteristics in iron–boron alloys. Journal of Alloys and Compounds, 819.

17. Xu, H., Zhu, W., Tang, M., Wang, X., & Zhang, Y. (2022). Effect of Bi_2O_3 on the structural and optical features of Co-doped Dy^{3+}/Eu^{3+} borofluorbismuth glass for white LED. Materials Today Chemistry, 26, 101074.

18. Berger, M. J., Hubbell, J. H., Seltzer, S. M., Chang, J., Coursey, J. S., Sukumar, R., Zucker, D. S., & Olsen, K. (2010). XCOM: Photon Cross Sections Database (NIST Standard Reference Database 8 – XGAM). National Institute of Standards and Technology (NIST).

19. Saleh, A. (2022). Comparative shielding features for X-/gamma-rays, fast and thermal neutrons of some gadolinium silicoborate glasses. Progress in Nuclear Energy, 154, 104482.

20. Issa, S. A. M., Tekin, H. O., Elsaman, R., Kilicoglu, O., Saddeek, Y. B., & Sayyed, M. I. (2018). Radiation shielding and mechanical properties of Al_2O_3–Na_2O–B_2O_3–Bi_2O_3 glasses using MCNP5 Monte Carlo code. Materials Chemistry and Physics, 223, 209–219.

21. Tekin, H. O., Sayyed, M. I., & Issa, S. A. M. (2018). Gamma radiation shielding properties of the hematite–serpentine concrete blended with WO_3 and Bi_2O_3 micro and nanoparticles using MCNPX code. Radiation Physics and Chemistry, 150, 95–100.

22. Sayyed, M. I., Issa, S. A. M., Tekin, H. O., & Saddeek, Y. B. (2018). Comparative study of gamma-ray shielding and elastic properties of BaO–Bi_2O_3–B_2O_3 and ZnO–Bi_2O_3–B_2O_3 glass systems. Materials Chemistry and Physics, 217.

23. Agar, O., Khattari, Z. Y., Sayyed, M. I., Tekin, H. O., Al-Omari, S., Maghrabi, M., et al. (2019). Evaluation of the shielding parameters of alkaline earth-based phosphate glasses using MCNPX code. Results in Physics, 12, 101–106.

24. Hine, G. J., & Brownell, G. L. (Eds.). (2013). Radiation Dosimetry. Elsevier.

25. Tonguc, B. T., Arslan, H., & Al-Buriahi, M. S. (2018). Studies on mass attenuation coefficients, effective atomic numbers, and electron densities for some biomolecules. Radiation Physics and Chemistry, 153, 86–91.

26. Al-Buriahi, M. S., Eke, C., Alomairy, S., Mutuwong, C., & Sfina, N. (2021). Micro-hardness and gamma-ray attenuation properties of lead iron phosphate glasses. Journal of Materials Science: Materials in Electronics, 32(10), 13906–13916.

27. Agar, O., Tekin, H. O., Sayyed, M. I., Korkmaz, M. E., Culfa, O., & Ertugay, C. (2019). Experimental investigation of photon attenuation behaviors for concretes including natural perlite mineral. Results in Physics, 12, 237–243.

28. Dong, M. G., Xue, X. X., Singh, V. P., Yang, H., Li, Z. F., & Sayyed, M. I. (2018). Shielding effectiveness of boron-containing ores in Liaoning province of China against gamma rays and thermal neutrons. Nuclear Science and Technology, 29(4), 1–8.

29. Lakshminarayana, G., Elmahroug, Y., Kumar, A., Dong, M. G., Lee, D. E., Yoon, J., & Park, T. (2020). TeO_2–B_2O_3–ZnO–La_2O_3 glasses: γ-ray and neutron attenuation characteristics analysis by WinXCOM, MCNP5, Geant4, and Penelope simulation codes. Ceramics International, 46(10), 16620–16635.

30. Makishima, A., & Mackenzie, J. D. (1973). Direct calculation of Young's modulus of glass. Journal of Non-Crystalline Solids, 12(1), 35–45.

31. ANSI/ANS-6.4.3 (W2001). (1991). Geometric progression gamma-ray buildup factor coefficients. American Nuclear Society.

32. Bashter, I. I. (1997). Calculation of radiation attenuation coefficients for shielding concretes. Annals of Nuclear Energy, 24(17), 1389–1401.

33. Kaur, P., Singh, K. J., Thakur, S., Singh, P., & Bajwa, B. S. (2019). Investigation of bismuth borate glass system modified with barium for structural and gamma-ray shielding properties. Spectrochimica Acta Part A: Molecular and Biomolecular Spectroscopy, 206, 367–377.

34. Al-Buriahi, M. S., Sriwunkum, C., & Boukhris, I. (2021). X- and gamma rays attenuation properties of DNA nucleobases by using FLUKA simulation code. European Physical Journal Plus, 136, 776.

35. Saeed, A., et al. (2021). Neutron and charged particle attenuation properties of volcanic rocks. Radiation Physics and Chemistry, 184, 109454.

36. Alothman, M. A., Olarinoye, I. O., Sriwunkum, C., Alomairy, S., & Alzahrani, J. S., Al-Buriahi, M. S. (2022). Study of the radiation attenuation properties of MgO–Al_2O_3–SiO_2–Li_2O–Na_2O glass system. Journal of the Australian Ceramic Society, 58(1), 267–273.

37. Alzahrani, J. S., Alrowaili, Z. A., Saleh, H. H., Hammoud, A., Alomairy, S., Sriwunkum, C., & Al-Buriahi, M. S. (2021). Synthesis, physical, and nuclear shielding properties of novel Pb–Al alloys. Progress in Nuclear Energy, 142.

38. Alharshan, G. A., Eke, C., & Al-Buriahi, M. S. (2022). Radiation-transmission and self-absorption factors of P_2O_5–SrO–Sb_2O_3 glass system. Radiation Physics and Chemistry, 193.

39. Al-Buriahi, M. S., Eke, C., Alrowaili, Z. A., Al-Baradi, A. M., Kebaili, I., & Tonguc, B. T. (2022). Optical properties and radiation shielding performance of tellurite glasses containing Li_2O and MoO_3. Optik, 249.

40. Al-Hadeethi, Y., Sayyed, M. I., & Al-Buriahi, M. S. (2020). Bioactive glasses doped with TiO_2 and their potential use in radiation shielding applications. Ceramics International, 46(10), 14721–14732.

41. Kilicoglu, O., & Tekin, H. O. (2020). Bioactive glasses and direct effect of increased K_2O additive for nuclear shielding performance: A comparative investigation. Ceramics International, 46(2), 1323–1333.

42. Al-Buriahi, M. S., et al. (2021). Newly developed glasses containing Si/Cd/Li/Gd and their high performance for radiation applications: Role of Er_2O_3. Journal of Materials Science: Materials in Electronics, 32, 9440–9451.

43. Olarinoye, I. O., et al. (2020). The effects of La_2O_3 addition on mechanical and nuclear shielding properties for zinc borate glasses in Monte Carlo simulation. Ceramics International, 46(18), 29191–29198.

44. Al-Buriahi, M. S., Sriwunkum, C., Arslan, H., Tonguc, B. T., & Bourham, M. A. (2020). Investigation of barium borate glasses for radiation shielding applications. Applied Physics A: Materials Science and Processing, 126(1).

45. Alyousef, H. A., Alotiby, M. F., Tijani, S. A., & Alotaibi, B. M. (2023). A study on the use of PMMA–Bi_2O_3 polymer composites as a replacement for concrete and gypsum at diagnostic photon energies. Journal of Radiation Research and Applied Sciences, 16(4), 100707.

46. Khan, N., Rooh, G., Mukamil, S., Khattak, S. A., Shoaib, M., Khan, I., Ullah, I., Ahmad, T., Shah, S. K., Safeen, K., & Shoaib, M. (2024). Radiation shielding performance of tellurium–thallium and tellurium–lead oxide glass systems. Radiation Physics and Chemistry, 217.

47. Saad, M., ALMohiy, H., Alshihri, A. A., Alqahtani, M. S., & Shalaby, R. M. (2023). Structural, mechanical, and radiation shielding properties of lead and lead-free alloys doped with CuO nanoparticles for radiation protection. Radiation Effects and Defects in Solids, 178(7–8), 1025–1037.

دراسة محاكاة: أداء الحماية من الإشعاع لزجاج البورو – فلور – بزموث المطعم بعناصر Dy/Eu

عبدالمنعم أحمد صالح[1] و بسمة محمد محمود[2]

[1] قسم العلوم الأساسية، المعهد العالي للتكنولوجيا، مدينة العاشر من رمضان، مصر

[2] قسم الفيزياء، كلية العلوم، جامعة سوهاج، مصر

يهدف هذا البحث إلى دراسة تأثير التغيير في تركيزات أكسيد البزموت (Bi_2O_3) وأكسيد الألومنيوم (Al_2O_3) على خصائص الحجب من أشعة جاما والنيوترونات في الزجاج. تم تحضير خمس عينات زجاجية بتركيب كيميائي $50B_2O_3 - (25-x)Al_2O_3 - 10Na_2O - xBi_2O_3 - 15CaF_2 - 0.5Dy_2O_3 - 0.5Eu_2O_3$ حيث x تأخذ القيم 5، 10، 15، 20، 25 مول. وتم حساب الخصائص الفيزيائية للزجاج محل الدراسة، مثل الحجم المولاري وكثافة التعبئة الذرية. أُستخدام كود مونتو كارلو (MCNP5)وبرنامج XCOM لإجراء الحسابات النظرية لدراسة خصائص الحجب، مثل معامل التوهين الكتلي(MAC) ، طبقة نصف القيمة(HVL) ، متوسط المسار الحر(MFP) ، والمقطع العرضي لإزالة النيوترونات (RCS) في مدى طاقي 15–15000 كيلو ألكترون فولت.

أظهرت النتائج أن زيادة تركيز Bi_2O_3 تؤدي إلى تحسين كبير في جميع الخصائص المذكورة، مما يجعل أن العينة المُشار إليها برمز S5 هي الأفضل من بين العينات محل الدراسة، إذ توفر حماية كاملة من الأشعة السينية (كفاءة الحماية الإشعاعية 100%). مقارنةً بمواد حجب أخرى، يُعد هذا الزجاج درعًا عالي الكفاءة للحماية من أشعة جاما والنيوترونات، مما يجعلها مناسبة للاستخدام في تطبيقات الحماية من الإشعاع.